Pergamon

Available online at www.sciencedirect.com
SCIENCE DIRECT®

Cement and Concrete Research 33 (2003) 957–964

CEMENT AND CONCRETE RESEARCH

The hydration characteristics of MSWI fly ash slag present in C_3S

K.L. Lin[a,*], K.S. Wang[b], T.Y. Lee[b], B.Y. Tzeng[b]

[a]*Environmental Engineering, National I-Lan Technology College, I-Lan 260, Taiwan*
[b]*Graduate Institute of Environmental Engineering, National Central University, Chung-Li 320, Taiwan*

Received 17 November 2001; accepted 20 September 2002

Abstract

This paper reports on an investigation of the hydration characteristics of C_3S and the mixing of C_3S with municipal solid waste incinerator (MSWI) fly ash slag. The results can be summarized as follows: TGA observations show lower amounts of CSH and $Ca(OH)_2$ in samples that incorporated MSWI slag into C_3S, possibly due to the partial replacement of the C_3S by slag with less activity. In general, the incorporation of slag into C_3S decreases the initial hydration reactions, but it increases the pozzolanic reactions at a later stage by consuming $Ca(OH)_2$. As the hydration precedes, the C_3S peaks decrease, up to 90 days, due to the activation of the slag by liberated $Ca(OH)_2$. As well, the amount of hydration products ($Ca(OH)_2$) from the pure C_3S pastes are more than for the C_3S-slag pastes. Moreover, the degree of hydration of the C_3S pastes increases with the curing time, the C_3S-slag paste also shows that lower hydration degree values at all ages.

Keywords: MSWI fly ash; Pozzolanic reaction; Hydration degree; Incorporation; Activation

1. Introduction

According to the ROC EPA statistical data from 1998, the amount of waste is increasing steadily by a growth rate of 5% annually in Taiwan. The incineration rate should reach 75% after 36 planned municipal solid waste incinerators (MSWIs) are finished in 2004 [1]. There will then be more than 3000 metric tons of incinerated fly ash and bottom ash to be dealt with per day. The disposal of MSWI ashes, in particular, heavy metal-containing fly ash, has become a significant continuing issue facing our society, both environmentally and economically. In general, these hazardous types of fly ash have to be detoxified, or stored in expensive secure landfills [2]. However, in response to a zero emissions goal as part of a sustainable waste disposal solution, MSWI fly ash that has been processed by melting offers not only an alternative to detoxification, but also the possibility of its being recycled as construction material (mainly fine aggregates) [3]. During the ash melting process, heavy metals and inorganic components in the ash are bound up molecularly into a glassy matrix [4], resulting in a chemically stable and physically durable product that is normally nontoxic in the natural environment [5]. However, in the alkaline environment of ordinary Portland cement, the fly ash derived slag becomes, in fact, chemically active, exhibiting self-cementing properties when pulverized and activated by the cement [6]. In other words, the pulverized slag is a latent hydraulic material, and could thus be utilized as a cement replacement in blends [7], or as an eco-cement. Thus, the melting of MSWI fly ash to make slag blended cement could not only resolve both detoxification and disposal problems, but also provide the means to utilizing the recovered ash as construction material. However, MSWI fly ash is often classified as hazardous, and in order to provide physical property analyses and a safety evaluation of masonry units made from such ash-blended cement, the hydraulic activity and the heavy metal leachability of the blends must be known.

Portland cement is a mixture with four principal constituents: C_3S (Ca_3SiO_5) 50–70 wt.%, C_2S (Ca_2SiO_4) 20–30 wt.%, C_3A ($Ca_3Al_2O_6$) 5–12 wt.% and C_4AF ($Ca_4Al_2Fe_2O_{10}$) 5–12 wt.% [8]. To gain better insights into the hydraulic characteristics of C_3S in MSWI slag, it is desirable to separately investigate the MSWI slag and its major compounds. There are very few publications concerned with the hydration of MSWI slag incorporated into C_3S.

* Corresponding author. Tel.: +886-3-935-7400; fax: +886-3-935-9674.
E-mail address: kllin@mail.ev.ncu.edu.tw (K.L. Lin).

0008-8846/02/$ – see front matter © 2002 Elsevier Science Ltd. All rights reserved.
doi:10.1016/S0008-8846(02)01002-5

Therefore, the present work is aimed at studying the hydration of MSWI slag incorporated into C_3S. All the hydration products were investigated using differential thermal and thermogravimetric analysis (DTA/TGA) as well as X-ray diffraction (XRD) techniques. The hydration degree was also studied by ^{29}Si MAS/NMR (^{29}Si nuclear magnetic resonance) techniques.

2. Materials and methods

2.1. Preparation of MSWI fly ash slag

The fly ash used in this study was collected from the cyclone of a mass-burning incinerator located in the northern part of Taiwan. The incinerator, capable of processing 1350 metric tons of local municipal solid waste per day, is equipped with air pollution control devices (APCD) consisting of a cyclone, an adsorption reactor, and a fabric baghouse filter. The fly ash was homogenized, oven dried at 105 °C for 24 h, and then its chemical composition was characterized. The major components in the ash are shown in Table 1. The ash has a basicity (defined as CaO/SiO_2) of 0.6, and a pouring point of approximately 1400 °C.

The MSW fly ash slag was prepared by melting the above cyclone ash in a 20-l electric-heated melter at 1400 °C for 30 min. The melts were water-cooled to obtain fine slag, which was then ground in a ball mill until fine enough to pass through a #200 sieve. The resultant pulverized slag has a fineness (on Blaine) of approximately 500 m^2/kg, with a specific gravity of 2.7.

Anhydrous C_3S was provided by the Construction Technology Laboratories, Skokie, IL, USA. C_3S was used as the binding agent in this study. Its chemical compositions are listed in Table 1.

Table 1
Chemical composition of C_3S, MSWI fly ash and slag

Composition	C_3S[a]	MSWI fly ash	MSWI fly ash slag
CaO (%)	72.3	16.6	27.3
SiO_2 (%)	25.2	34.3	38.9
Al_2O_3 (%)	0.08	4.3	23.3
Fe_2O_3 (%)	0.02	3.6	5.4
MgO (%)	<0.01	0.5	3.6
SO_3 (%)	<0.01	8.8	0.2
Na_2O (%)	<0.01	5.3	1.3
K_2O (%)	<0.01	3.0	<0.01
TiO_2 (%)	0.01	4.2	–
P_2O_5 (%)	<0.01	3.9	–
Mn_2O_3 (%)	0.01	–	–
SrO (%)	<0.01	–	–
Zn (mg/l)	–	7115	6480
Pb (mg/l)	–	1284	295
Cu (mg/l)	–	1409	604.4
Cr (mg/l)	–	811	695.3
Cd (mg/l)	–	80	5.8

[a] Construction Technology Laboratories, Skokie, IL, USA.

2.2. Paste tests

Slag blended C_3S pastes (C_3S-slag) consisting of 80% C_3S and 20% pulverized slag were compared to a blend of 100% C_3S. A water to binder ratio of 0.38 was used for both mixtures. Test cubes of $25.4 \times 25.4 \times 25.4$ mm ($1 \times 1 \times 1$ in.) were prepared according to ASTM-305, followed by demoulding (ASTM C31-69), then cured in an environmental chamber, maintained at 25 °C with a relative humidity >98%, for periods ranging from 1 to 90 days. After curing for 1, 3, 7, 14, 28, 60 or 90 days, the samples were subsequently crushed and the hydration reactions were stopped with absolute alcohol, filtrated in vacuum, washed with acetone for several times and dried, then subjected by XRD, DTA/TGA and ^{29}Si nuclear magnetic resonance analyses.

2.3. Analytical methodology

The major analyses performed on the C_3S-slag pastes and its cubes included TCLP, and chemical composition determination as follows:

- TCLP: SW 846-1311.
- Chemical composition: inductively coupled plasma-atomic emission spectrometer (ICP-AES).
- Leaching concentration: Cd (SW846-7131A), Pb (SW846-7421), Zn (SW846-7951), Cu (SW846-7211), Cr (SW846-7191).
- XRD: the XRD analyses were carried out by a Siemens D-5000 X-ray diffractometer with CuKα radiation and 2θ scanning, ranging between 5° and 70°. The XRD scans were run at 0.05° steps, with a 1-s counting time.
- DTA/TGA: DTA/TGA analyses of the samples were performed using a Seiko SSC Model 5000 Thermal analyzer. Dry N_2 gas was used as a stripping gas and a heating rate of 0.5 °C was used. The samples were heated from 25 to 1000 °C.
- Chemical shift of linear polysilicate anions in C–S–H: ^{29}Si MAS/NMR.

The degree of hydration of pure C_2S and C_3S-slag pastes, and the average length of linear polysilicate anions in the calcium silicate hydrate (CSH) gels, primarily responsible for the strength, were analyzed by using high resolution solid state ^{29}Si MAS/NMR techniques as follows.

The increase of diamagnetic shielding to the ^{29}Si nuclei that resulted from the degree of increasing condensation from the single tetrahedral structure of the monosilicates (Q^0) to the end groups (Q^1), to the chain middle groups (Q^2), to the layers and branching sites (Q^3), and finally to the three-dimensional frameworks (Q^4), led to well-separated and analytically useful chemical shift ranges for each type of SiO_4 unit [9,10]. That is, the calcium silicate hydrates, the hydration products in the cement, could be semiquantified

Table 2
Range of ^{29}Si chemical shifts of Q^n units in solid silicates

Types of Si–O–X group	Symbol	Range (ppm)
Monosilicates	Q^0	−68 to −76
Disilicates and chain end group	Q^1	−76 to −82
Chain middle groups	Q^2	−82 to −88
Chain branching sites	Q^3	−88 to −92
Three-dimensional framework	Q^4	−92 to −129

using chemical shifts in the ^{29}Si nuclei in the Si–O–X groups, for which the structures are shown below [11]:

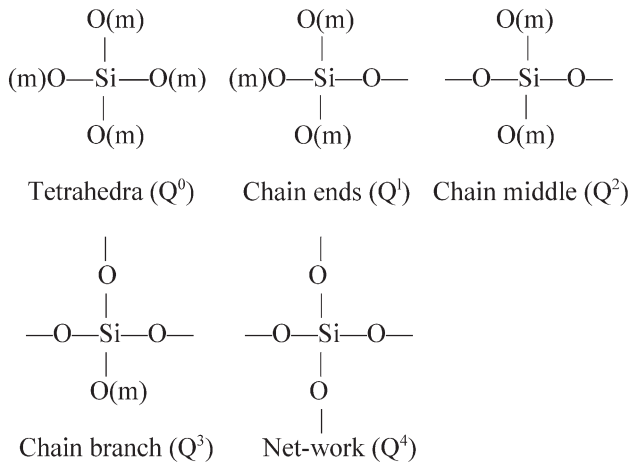

High-resolution ^{29}Si MAS/NMR spectra were recorded at 39.72 MHz on an MSL Bruker MAS/NMR-200 solid-state high-resolution spectrometer, using rapid (about 3 kHz) sample spinning at the magic angle to the external magnetic field. The ^{29}Si chemical shifts are given relative to the primary standard liquid tetramethylsilane (TMS) in the delta-scale (the negative signs correspond to up-field shifts). The sharp ^{29}Si signal chemical shifts for the above S–O–X groups in solid silicates are summarized in Table 2.

The hydration degree (designated as α) of the cement clinkers, C_2S and C_3S, can be evaluated as follows by the integral intensity of the signals at −70 ppm (Q^0) for both the hydrated cement paste and cement powders, i.e., $I^0(Q^0)$ and $I(Q^0)$, respectively [8]:

$$\alpha(\%) = 100 - [I(Q^0)/I^0(Q^0)]100 \quad (1)$$

3. Results and discussion

3.1. Characterization of MSWI fly ash and slag

Table 1 lists the major components of the MSW slag used in this study. The XRD patterns of the MSWI fly ash and slag are shown in Fig. 1. Fig. 1 shows the speciation in the fly ash, as identified by the XRD techniques, indicated that the major compositions were composed of quartz (SiO_2), anhydrite ($CaSO_4$), gehlenite ($Ca_2Al_2SiO_7$), anorthite ($CaAl_2Si_2O_8$), microcline ($KAlSi_3O_8$), calcium chloride ($CaCl_2$), $CaCl_2{\cdot}Ca(OH)_2{\cdot}H_2O$, Sylvite (KCl) and Halite (NaCl). Fig. 1 shows the slag contains large amounts of glass, which is indicated by the broad diffuse bands between 24° to 37° (2θ).

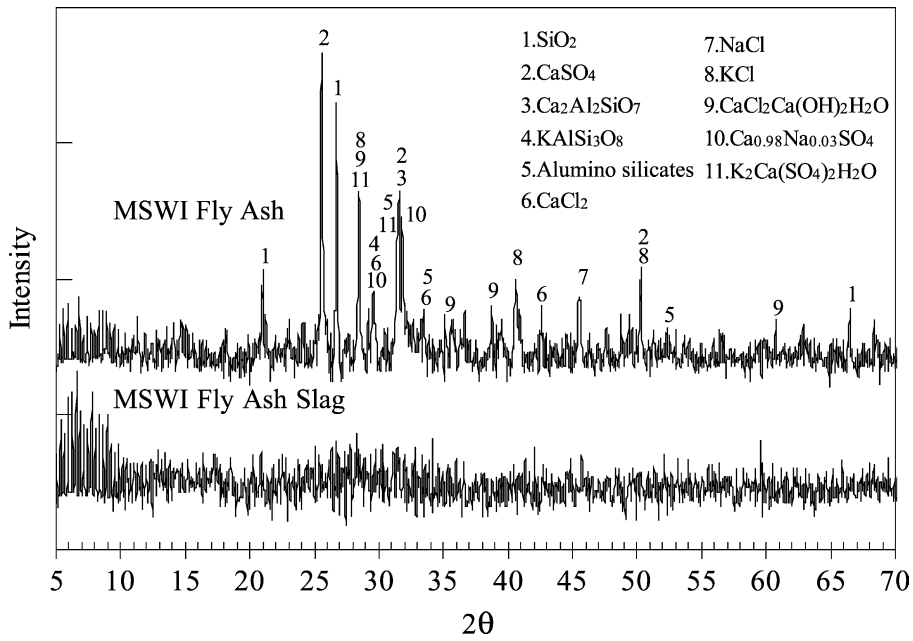

Fig. 1. The XRD patterns of MSWI fly ash and slag.

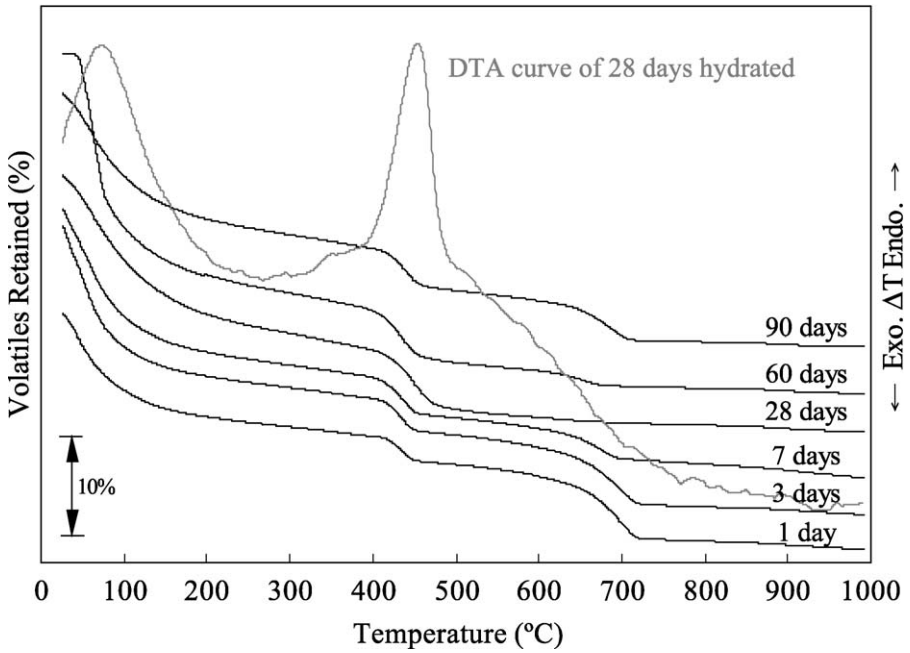

Fig. 2. Thermogravimetric and differential thermal analysis of hydrated C_3S paste.

3.2. DTA/TGA of C_3S and C_3S-slag pastes

The hydration products of both pure C_3S and C_3S-slag pastes for 28 days can be seen in Figs. 2 and 3, respectively. The DTA curves for C_3S pastes cured from 1 to 90 days showed two endothermic effects, at 100–200 and 400–480 °C (Fig. 2). Taylor [12] has reported mass loss for CSH, due to dehydration reactions, at 100–200 °C. The hypothesis that C_3S hydrates with the liberation of $Ca(OH)_2$. The $Ca(OH)_2$ reacts with active silica constituents of MSWI fly ash slag to form CSH. The second peak can be attributed to the decomposition

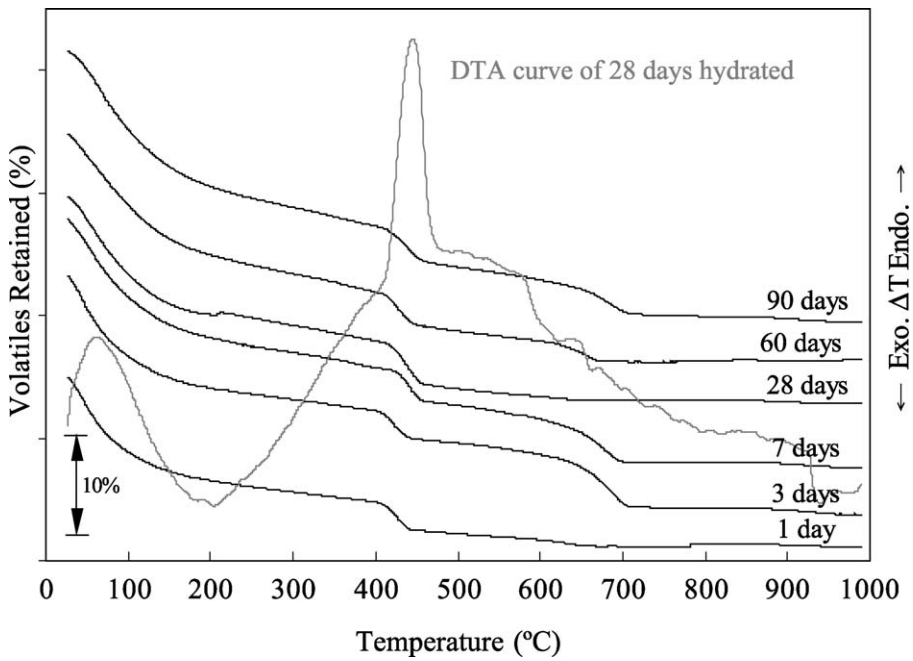

Fig. 3. Thermogravimetric and differential thermal analysis of hydrated C_3S-slag paste.

Table 3
The mass loss during the TG analysis of pure C_3S and C_3S-slag pastes

Samples	Curing time (day)	Weight loss (%)	
		CSH	$Ca(OH)_2$
C_3S	1	2.60	2.13
	3	2.65	2.51
	7	2.65	2.98
	28	3.61	5.61
	60	3.81	3.62
	90	3.93	3.61
C_3S-slag	1	2.17	2.01
	3	2.31	2.44
	7	2.31	2.97
	28	3.56	4.29
	60	3.79	2.97
	90	3.85	2.88

of $Ca(OH)_2$. Table 3 indicates that as the hydration proceeds up to 90 days, the amount of CSH increases. It can be seen that pure C_3S becomes hydrated by producing $Ca(OH)_2$, which increases over time up to 28 days, then decreases up to 90 days.

Fig. 3 shows results of the thermogravimetric analysis of C_3S-slag pastes. It also illustrates the endothermic effects at 100–200 and 400–480 °C. On the other hand, $Ca(OH)_2$ is formed in smaller amounts than for C_3S pastes. As hydration proceeds, the amount of CSH gel at 400–480 °C increases with time. Table 3 indicates that the C_3S-slag pastes have lower CSH and $Ca(OH)_2$ values than do the pure C_3S pastes, at all stages of hydration.

3.3. Changes of hydration products in the C_3S and C_3S-slag pastes

The hydration products of pure C_3S and C_3S-slag pastes, at the various curing times, can be seen in the XRD patterns in Figs. 4 and 5, respectively. The C_3S samples showed $Ca(OH)_2$ peaks up to 90 days and residual C_3S. From the XRD patterns of hydrated C_3S pastes, it is clear that the free calcium hydroxide increases up to 28 days, then slowly decreases at 90 days.

Fig. 5 shows the XRD patterns for hydrated C_3S-slag paste samples. $Ca(OH)_2$ peaks up to 90 days with residual C_3S. As the hydration proceeds, the C_3S peaks decrease, up to 90 days, due to the activation of the slag by liberated $Ca(OH)_2$. As well, the amount of hydration products from the C_3S-slag pastes are smaller than from pure C_3S pastes.

3.4. NMR analysis of C_3S and C_3S-slag pastes

Figs. 6 and 7 present the ^{29}Si MAS/NMR spectra of the hydrated samples of pure C_3S and C_3S-slag pastes at various stages. The results show the increased intensity of signals from Q^2 silicone sites in the hydrated, mechanically activated blends. It is known that the CSH formed by the hydration of calcium silicates is generally dominated by Q^1 sites or has abundant Q^1 and Q^2 sites. The ratio, Q^2/Q^1 of silicone sites in the hydrated products, also rises after the mechanical activation of the blends. The hypothesis that, in MSWI slag, thin SiO_2 layers form around C_3S crystals, which accelerates the pozzolanic reaction and promotes the growth of more extensive nets of hydrated products, is suggested.

These and the other results are summarized in Table 4. Table 4 indicates the hydration degree of pure C_3S pastes, as well as the C_3S-slag pastes, up to 90 days. The hydration degree of pure C_3S increases with time, up to 90 days. Also, C_3S-slag pastes show lower hydration degree values at all ages of hydration. The hypothesis

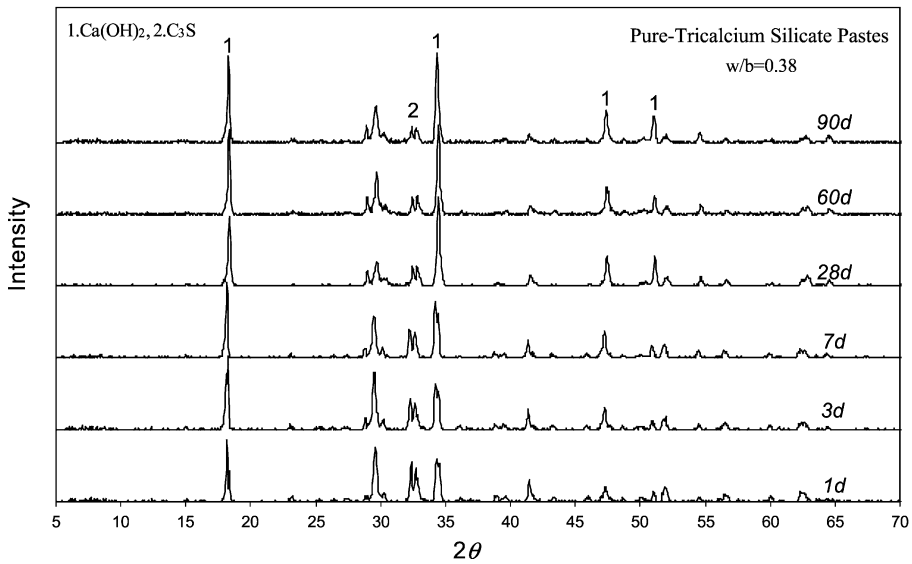

Fig. 4. X-ray diffraction patterns of hydrated C_3S pastes.

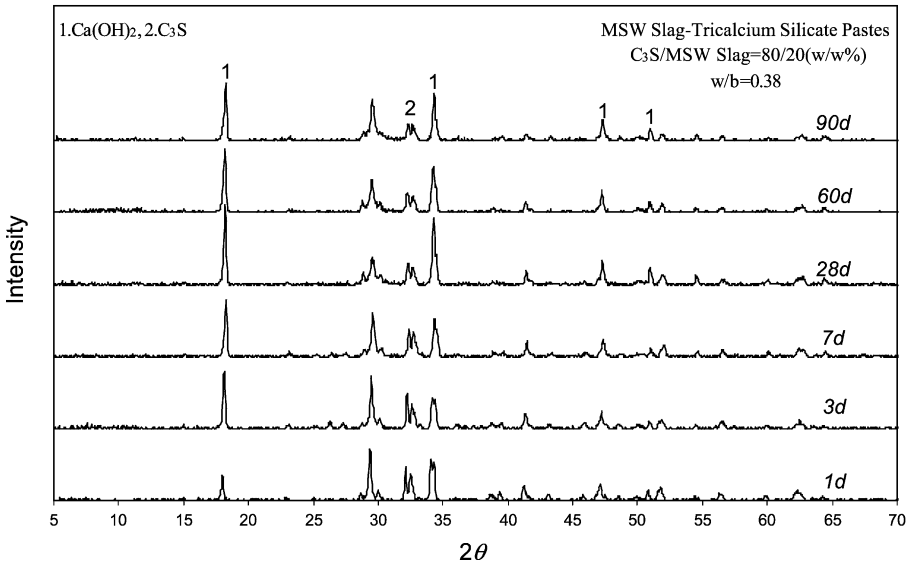

Fig. 5. XRD patterns of hydrated C_3S-slag pastes.

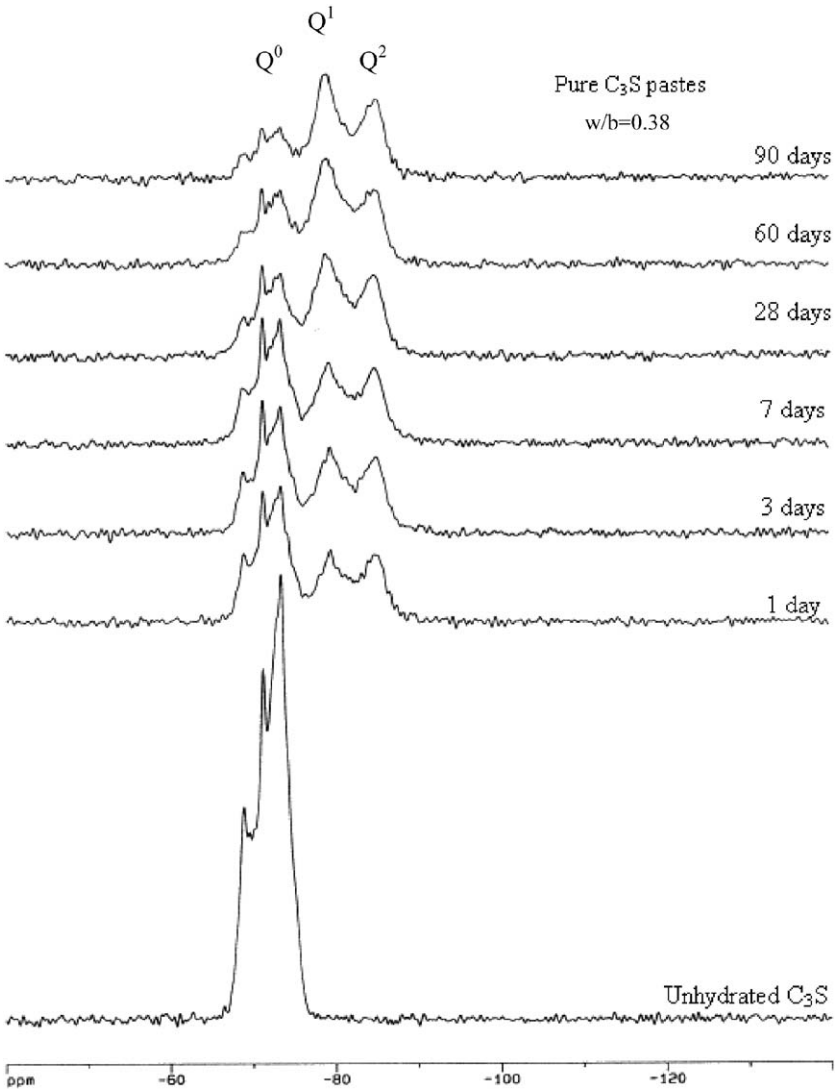

Fig. 6. ^{29}Si MAS/NMR spectra of hydrated C_3S pastes.

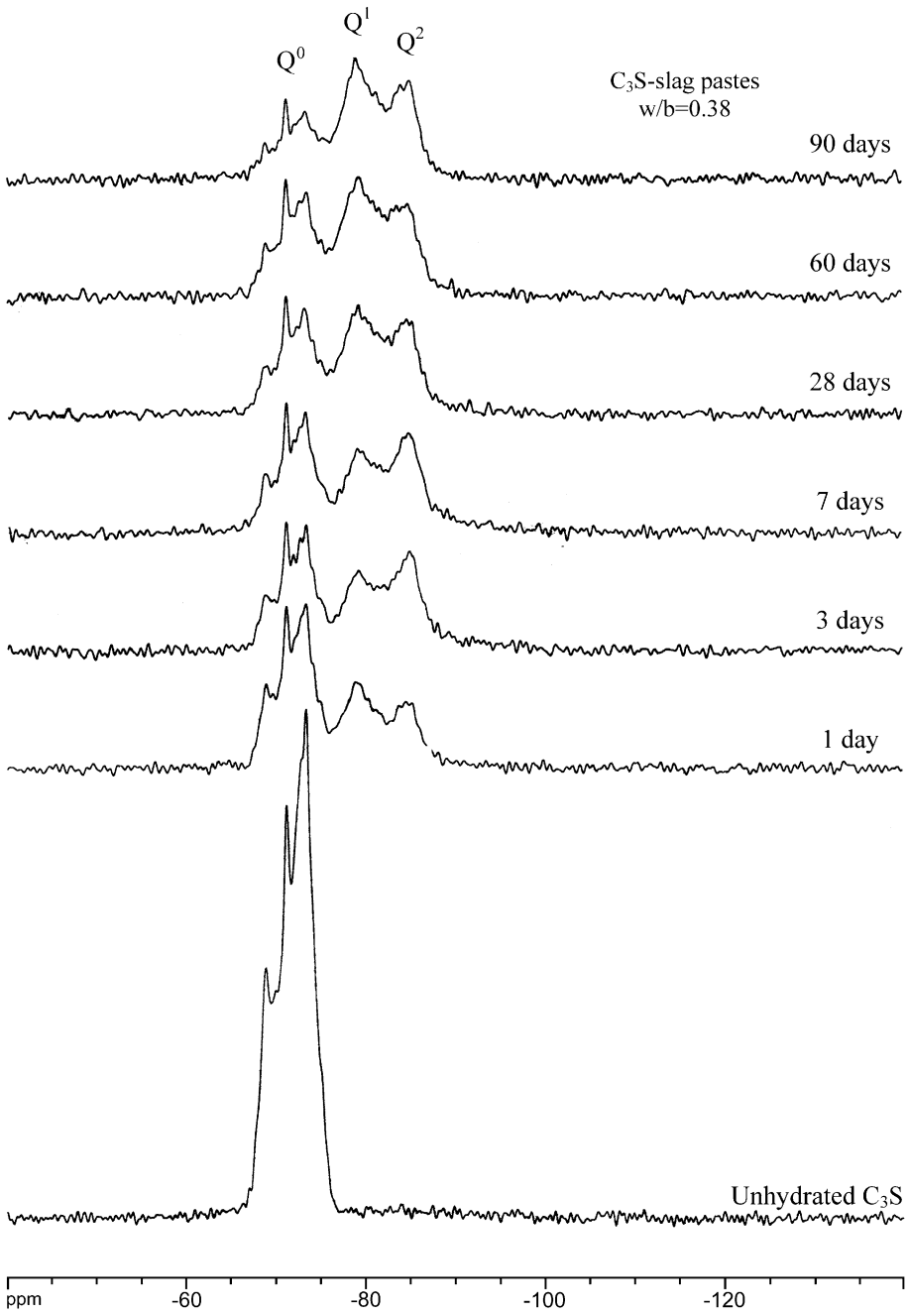

Fig. 7. ^{29}Si MAS/NMR spectra of hydrated C_3S-slag pastes.

that the sluggish behavior of slag formation of acidic film on the grains of slag that retards hydration [12].

4. Conclusions

This study investigates the hydration characteristics of pure C_3S pastes and C_3S-slag pastes. They can be summarized as follows:

1. The C_3S-slag pastes have lower CSH and $Ca(OH)_2$ values than the pure C_3S pastes at all stages of hydration, possibly due to the partial replacement of C_3S by slag with less activity.
2. As the hydration precedes, the C_3S peaks decrease, up to 90 days, due to the activation of the slag by liberated $Ca(OH)_2$. As well, the amount of hydration products ($Ca(OH)_2$) produced from the C_3S-slag pastes are smaller than from the pure C_3S pastes.
3. ^{29}Si MAS/NMR techniques indicate that the hydration degree of pure C_3S pastes increases with time; also C_3S-slag pastes show that the hydration degree values at all ages is lower.

Table 4
^{29}Si NMR analysis for slag blended monoliths for different curing times

Samples	Curing time (day)	^{29}Si NMR integral intensities of Q^n						Hydration degree (%)
		Q^0	Q^1	Q^2	Q^3	Q^4	Total	
C_3S	Unhydrated	981	11	4	1	3	1000	–
	1	553	264	169	2	12	1000	43.6
	3	488	288	190	16	18	1000	51.2
	7	478	299	201	10	12	1000	52.2
	28	391	355	249	0	5	1000	60.9
	60	344	373	265	9	9	1000	65.6
	90	292	405	299	5	0	1000	70.8
C_3S-slag	1	570	222	145	34	29	1000	32.1
	3	465	280	190	34	31	1000	44.6
	7	440	294	200	38	28	1000	47.6
	28	377	335	239	26	23	1000	55.1
	60	364	352	256	16	13	1000	56.7
	90	298	391	297	13	0	1000	64.5

References

[1] W.F. Yang, Report of Department of Environmental Protection, Taipei Municipal Government, ROC EPA, 1999.
[2] F.G. Simon, In RecTM process for recovering material from solid waste incineration residues, Resid. Treat., ABB Rev. 6 (1995) 15–20.
[3] J.I. Bhatty, K.J. Reid, Compressive strength of sludge ash mortars, ACI Mater. J. 86 (M34) (1989) 394–400.
[4] S.I. Abe, F. Kambayashi, M. Okada, Ash melting treatment by rotating type surface melting furnace, Waste Manage. 16 (1996) 431–443.
[5] S. Mindess, J.F. Young, Concrete, Prentice-Hall, New Jersey, 1981.
[6] P.K. Mehta, Concrete, Prentice-Hall, New Jersey, 1986.
[7] J. Pera, A. Wolde, C. Michel, Hydraulic activity of slags obtained by vitrification of wastes, ACI Mater. J. 93 (M70) (1996) 613–618.
[8] C.K. Lin, J.N. Chen, C.C. Lin, An NMR, XRD and EDS study of solidification/stabilization of chromium with Portland cement and C_3S, J. Hazard. Mater. 56 (1997) 21–34.
[9] J. Hjorth, ^{29}Si MAS/NMR studies of Portland cement components and effects of microsilica on the hydration reaction, Cem. Concr. Res. 18 (1988) 788–798.
[10] G. Engelhardt, D. Michel, High-Resolution Solid-State NMR of Silicates and Zeolites, Wiley, New York, 1987.
[11] H. Justnes, I.M. Bjoergum, J. Krane, T. Skjetne, NMR—A powerful tool in cement and concrete research, Adv. Cem. Res. 30 (11) (1990) 105–113.
[12] H.F.W. Taylor, Cement Chemistry, Academic Press, New York, 1997.